Physico-Chemical and Structural Characterization of Mixed Natural Polymer Hydrogels Under Simulated Gastrointestinal Fluid

Agustina Ari Murti Budi Hastuti[1,2]*, Khadijah Zai[3], Puput Risdanareni[4], Rahmi Karolina[5] and Irfan Mustafa[6]

1. Department of Pharmaceutical Chemistry, Faculty of Pharmacy, Universitas Gadjah Mada, Yogyakarta 55281, Indonesia
2. Center of Excellence Institute for Halal Industry and Systems (PUI-PT IHIS), Universitas Gadjah Mada, Yogyakarta 55281, Indonesia
3. Department of Pharmaceutics, Faculty of Pharmacy, Universitas Gadjah Mada, Yogyakarta 55281, Indonesia
4. Department of Civil Engineering, Faculty of Engineering, State University of Malang, Semarang Street 5, Malang 65145, Indonesia
5. Civil Engineering Department, Faculty of Engineering, Universitas Sumatera Utara, Indonesia
6. Department of Biology, Faculty of Mathematics and Natural Sciences, Universitas Brawijaya, Malang 65145, Indonesia

Article Info	ABSTRACT
	Functional food components are vital for preserving health and avoiding illnesses by supplying necessary nutrients and maintaining physiological equilibrium. Nevertheless, the efficient distribution of these substances is impeded by obstacles such as limited solubility and stability, particularly in the gastrointestinal system. Integrating these elements into hydrogel beads offers a viable approach to improve their absorption. This work investigated the synthesis of hydrogel beads by combining four natural polymers: carboxymethyl cellulose (CMC), alginate, chitosan, and guar gum. The hydrogel was formed by crosslinking aided with calcium chloride. The hydrogels were characterized by swelling tests, Fourier-transform infrared spectroscopy (FTIR), and scanning electron microscopy (SEM). Experiments conducted using simulated gastric and intestinal fluids showed that some formulations are appropriate for delivering nutrients to certain parts of the gastrointestinal tract. The FTIR analysis revealed clear characteristics of each polymer and their combinations in the hydrogel compositions. The hydrogel beads' morphological features were revealed by SEM imaging. This work offers valuable information on how to develop hydrogels as carriers for effectively delivering nutrients into the gastrointestinal system. It also proposes potential areas for further investigation in integrating active substances into hydrogel matrices. **Keywords:** hydrogel, functional food, swelling, FTIR, SEM

INTRODUCTION

Functional food components, such as vitamins and vitaminoids, minerals, prebiotics, and probiotics, etc., are contained in a healthy diet to provide nutrients, satisfy metabolic requirements, maintain physiological homeostasis, and protect against diseases. To meet daily nutritional needs, functional food components are often consumed as supplements. Some of the functional food components are challenging to formulate due to low solubility and poor stability, especially during their delivery in the gastrointestinal track. To overcome this problem, incorporation of functional food components into hydrogel beads is one strategy to improve delivery. Hydrogels, by definition, are cross-linked polymers containing covalent bonds, physical cross-links, association bonds, and/or crystallites that can absorb large amounts of water. Hydrogel can be formed by physical crosslinking (such as ionic or electrostatic interactions, hydrophobic interactions, thermal induction, ultrasound induction, crystallization, hydrogen bonding, or metal coordination) or chemical crosslinking (such as photopolymer-

ization, enzyme catalyzed reactions, "click-chemistry", or other chemical reactions) (Hu *et al.*, 2019).

Biodegradable hydrogels derived from natural polymers, deemed to be safer than synthetic ones, have been developed for the encapsulation of nutraceuticals and other bioactive compounds. Natural polymers are superior as they are biocompatible for humans, harmless for living tissues, and easily degradable (Rahman *et al.*, 2019). Carotenoids, for example, have been incorporated into calcium alginate beads to improve their delivery in the gastrointestinal track by preventing flocculation of the lipid droplets (Mun *et al.*, 2015). Encapsulated carotenoids are also more stable at low pH compared to those "free" carotenoids that are more prone to degradation (Zhang *et al.*, 2016). Curcumin-loaded polysaccharide-based hydrogel has the same benefit, as curcumin undergoes rapid degradation and is easily metabolized in the gastrointestinal track (Zhang *et al.*, 2016). Hydrogel beads can be optimized to release functional food components at specific areas along the gastrointestinal track due to their differential stability under different pH conditions (Zhang *et al.*, 2015; Zhang *et al.*, 2016).

A wide range of natural polymers can be used to encapsulate functional food components. Natural polymers are categorized into two groups, which are polysaccharides and proteins. Polysaccharides are made up of monosaccharides that are linked by glycosidic bonds. Polysaccharides can be derived from plants, such as alginate, cellulose, and guar gum, or from animals, such as chitosan, hyaluronic acid, and chondroitin (Liu *et al.*, 2021). Cellulose, the most abundant polymer in nature, has been widely used as polymers as the structure is easily manipulated by modification of the hydroxyl groups into various cellulose derivatives, resulting in wide range of application (Trombino *et al.*, 2009). Chitosan, derived from chitin, is the second most abundant polymer in nature. Chitosan is quite versatile, and its characteristics can be adapted according to the usage (Rahman *et al.*, 2019). Alginate is also a common polysaccharide to produce hydrogel due to the easiness to form ionic crosslinking. However, the hydrogel produced is mechanically weak and brittle, so that addition of another polymer is preferable (Ji *et al.*, 2022). Guar gum is a neutral polymer which consists of β−D−mannopyranose and α−d−galactopyranose. Similar to alginate, guar gum-based hydrogel has low strength and needs

other polymers to stabilize its structure (Pak & Chen, 2023). Protein polymers that are usually used as ingredients for making hydrogels also can be acquired from plants, such as glycinin and zein, or animals, such as gelatin, collagen, and elastin (Panahi & Baghban-Salehi, 2019). Hydrogels from single polymers usually have limited properties and capacities to deliver compounds, including water absorbing capacity and stability. Therefore, hydrogels are often made from a combination of two or more types of polymers to improve the desired properties (Liu *et al.*, 2021).

Evaluation of the performance and structure is helpful to determine the utilization of hydrogels. In addition to the native characteristics, the attributes of hydrogels are influenced by local environmental conditions such as pH, heat, pressure, ionic strength, solvent composition, etc. (Azeera *et al.*, 2019). The characterization of hydrogels requires various techniques, such as swelling performance and Fourier-transform infrared spectroscopy (FTIR) for the physico-chemical characterization and scanning electron microscopy (SEM) for the structural characterization. The swelling performance of hydrogel evaluates the ability to absorb water, either dynamically or in equilibrium. Hydrogels are considered porous, which is formed by the internal cross-linking and the presence of multiple hydrophilic groups. The swelling ratio is often determined by the ratio of water absorbed to the dry weight of the hydrogels (Azeera *et al.*, 2019). FTIR spectra identify functional groups of the hydrogels, which could differ from the individual polymers as starting materials (Gulrez *et al.*, 2011). Each type of material has a unique FTIR spectra known as a "fingerprint". The FTIR technique is non-destructive and often requires minimum to no sample preparation. SEM provides a morphological display of the hydrogel's surface. The SEM figures are useful to indicate the cross-linking of the hydrogels under different conditions.

In this study, we produced hydrogel beads with different combinations of CMC, alginate, chitosan, and guar gum (Figure 1). The hydrogel beads were subjected to buffered solutions of different pHs, similar to those of gastrointestinal fluid and characterized by swelling tests, FTIR, and SEM. This database can be used as a starting guide to formulate encapsulated materials intended for absorption in certain parts of the gastrointestinal track.
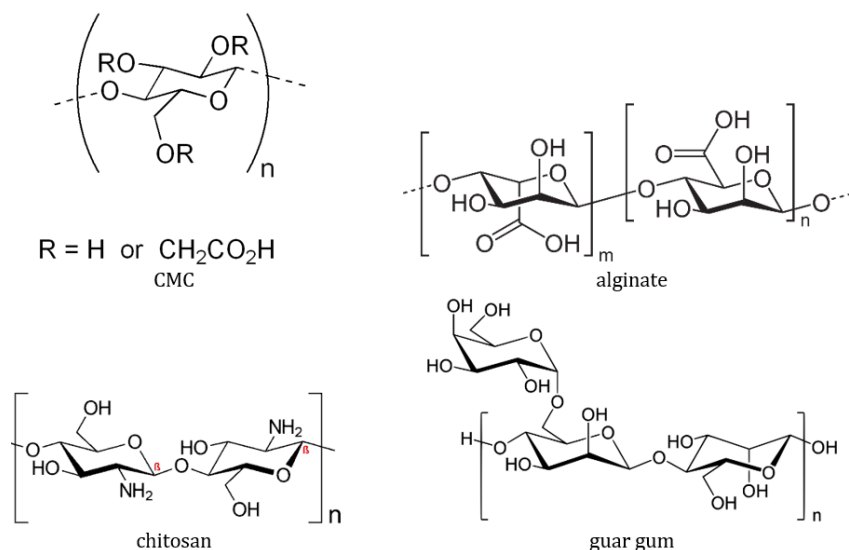
Figure 1. Molecular structure of CMC, alginate, chitosan, and guar gum

Table I. Composition of polymers to produce hydrogels. C=CMC, A=alginate, X=chitosan, G=guar gum.

Sample code	Percentage (%)			
	CMC	Alginate	Chitosan	Guar gum
C75A25	75	25	0	0
C50A25X25	50	25	25	0
C25A50X25	25	50	25	0
C25A25X50	25	25	50	0
C50A25G25	50	25	0	25
C25A50G25	25	50	0	25
C25A25G50	25	25	0	50
C50A25X12.5G12.5	50	25	12.5	12.5
C25A50X12.5G12.5	25	50	12.5	12.5
C25A25X25G25	25	25	25	25

MATERIALS AND METHODS

Four natural polymers were used in this research. CMC were produced by Changsu Wealthy Science and Technology Co., Ltd., Jiangsu, China. Alginate with a specification of loss on drying 10.0%, viscosity (1% solution) 180 mPas, pH (1% solution) 7.2, and particle size of less than 18 mm (Alginatos Chile S.A., Santiago, Chile). Chitosan was produced from blue crab shell (*P. pelagicus*) with particle size of less than 0.074 mm, moisture regain 9.04%, residue of ignition 0.889%, degree of deacetylation 96.19%, viscosity 74.99 mPas, molecular weight 168 kDa, protein content <0.2% (Chimultiguna, Indramayu, Indonesia). Guar gum with characteristics of moisture 8.19%, ash 0.78%, protein 4.20%, RIA 2.42%, galactomannan 84.11%, particle size less than 0.074 mm for 96.07% (Lucid Colloids Ltd., Mumbai, India). NaOH, acetic acid, and CaCl$_2$ were purchased from Merck KGaA (Darmstadt, Germany). Distilled water was locally produced by General Labora (Yogyakarta, Indonesia).

Hydrogels production

Hydrogels were produced with two to four combinations of natural polymers of CMC, alginate, chitosan, and/or guar gum (Table I). All stock solutions for single polymers were made by slowly adding polymer powder under stirring with a Stuart SS10 overhead stirrer (Cole-Parmer, Vernon Hills, IL, USA) until the polymer was wet and homogeneous with a final concentration of 1% for all polymers. The stock solution of CMC was made by adding 10 g CMC to 1000 mL of 0.1 M NaOH under stirring at 500 rpm at room temperature. An alginate stock solution was prepared by dissolving 10 g alginate in 1000 mL 0.1 M NaOH and stirring at 500 rpm at 45°C. A chitosan solution was made

by dissolving 10 g chitosan in 1% acetic acid under continuous stirring at room temperature to obtain pale-yellow viscous solution. A guar gum stock solution was made by adding 10 g guar gum to 1000 mL of water under stirring at 500 rpm at room temperature. Distilled water was used throughout the experiment.

Depending on the compositions (Table I) CMC was mixed with chitosan and stirred for 30 minutes at 300 rpm. After 10-minutes of rest, guar gum was added to the mixture and stirred for 30 minutes at 300 rpm. Lastly, 10-minutes-rest was needed before alginate was added to the mixture and stirred for 30 minutes at 300 rpm. The final product was rested for 30 minutes at room temperature. Afterwards, the combination of polymers was injected using a 20 ml syringe with a needle (Terumo Europe N.V., Leuven, Belgium) into a 2% $CaCl_2$ solution to induce hydrogel beads formation. After overnight incubation at room temperature, the resulting hydrogel beads were filtered and washed with distilled water to remove excess $CaCl_2$. The hydrogel beads were dried using an SP VirTis BenchTop Pro freeze dryer (SP Industries, Inc., Warminster, PA, USA) at 100 mT pressure.

Swelling performance test

The dried hydrogels were weighed and immersed in buffer solutions with different pH (HCl buffer at pH 2 and phosphate buffer at pH 6.8) at 25°C for 24 h. The swelling ratio was calculated from three replicates using the equation as follows:

$$Swelling\ ratio = \frac{W_t - W_0}{W_0}$$

wherein W_t and W_0 refer to the weight of swollen beads at t (10 min, 2 h, and 24 h) and 0 h, respectively.

Fourier-transform infrared spectroscopy (FTIR)

FTIR spectra was acquired using a Thermo Nicolet iS10 FTIR spectrometer equipped with a Smart iTR diamond ATR accessory (Thermo Fisher Scientific, Madison, USA). The sample was placed on the crystal window of the infrared spectrophotometer and pressed with a fixing clamp. The scanning was performed in the range of 4000-600 cm^{-1} with an interval of 0.964 cm^{-1} with 32 scans for every measurement. The sample window was cleaned with water and acetone in between samples, and the background collection was determined afterwards.

Scanning electron microscopy (SEM)

Prior to SEM imaging, the sample was placed on the carbon tape of the specimen holder for drying. The sample was then coated with Au using a JEOL JEC-3000FC auto fine coater (JEOL, Tokyo, Japan). The coating procedure was done for ± 120 s with vacuum coater pressure at ± 3.2 Pa. Imaging of the hydrogel was performed with a JEOL JSM-6510LA scanning electron microscope (JEOL, Tokyo, Japan). The sample was placed in the instrument and subjected to vacuum for ± 60 s. Electrons were shot at the samples at a certain probe level and the topography was recorded.

RESULTS AND DISCUSSION
Hydrogels production

Ten formulas (Table I) were successfully made into hydrogels. Ionic crosslinking by $CaCl_2$ facilitates the gelling processes of the hydrogels, in which the cross-linking density is affected by the concentration of $CaCl_2$. The increasing concentration of $CaCl_2$ reduces the swelling capacity of the hydrogel due to the increasing cross-linking of the hydrogel, making the structure more compact (Feyissa *et al*., 2023). The Ca^+ ions form ionic interactions with the negative charge of the polysaccharides. Therefore, the presence of alginate, which has a negative charge, in the formula increases the stability of the hydrogel (Çelik *et al*., 2016). The wet hydrogel beads immersed in $CaCl_2$ solution appear as whitish bubbles. The freeze-drying procedure takes around 3 to 4 days depending on the sample volume.

Swelling performance

The swelling performance was evaluated using HCl buffer pH 2 and phosphate buffer pH 6.8 to simulate gastric fluid and intestinal fluid, respectively. At pH 2, the swelling ratio ranges from 237.15±21.33% for hydrogel C25A50X12.5G12.5 to 1100.60±63.36% for hydrogel C25A25X25G25 at 10 mins (Figure 2). The swelling of all formulas is increased at 2 h. When evaluated after 24 h, the swelling of C50A25X25, C25A50X25, C25A50G25, C25A25G50, C25A50X12.5G12.5, and C25A25X25G25 did not differ much from those respective formulas at 2 h. The rest of the formula (C75A25, C25A25X50, C50A25G25, and C50A25X12.5G12.5) were digested at 24 h. Hydrogel immersed in phosphate buffer at pH 6.8 for 10 mins shows a swelling ratio ranging from 230.41±11.75% to 960.83±19.73% for hydrogel C25A50X12.5G12.5 and C50A25X25, respectively.
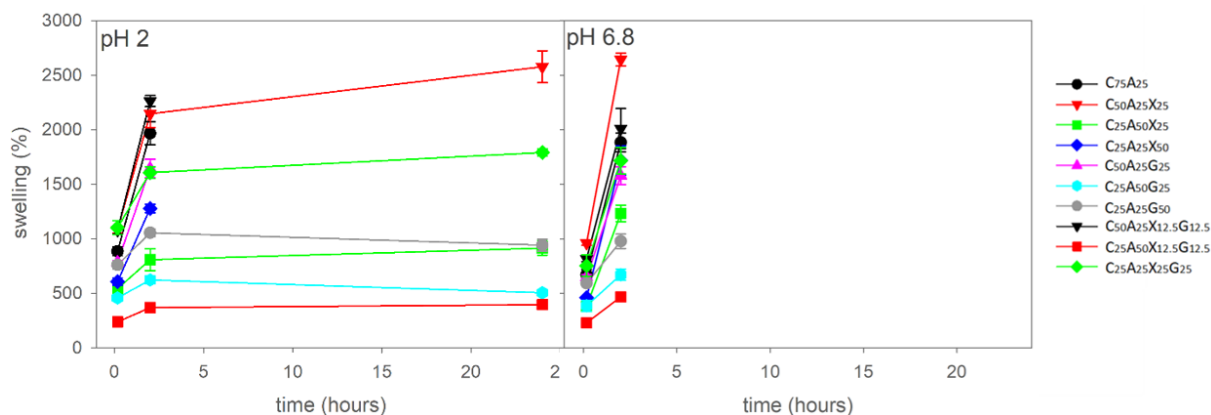
Figure 2. Swelling capacity of the hydrogels in immersed in HCl buffer pH 2 and phosphate buffer pH 6.8.
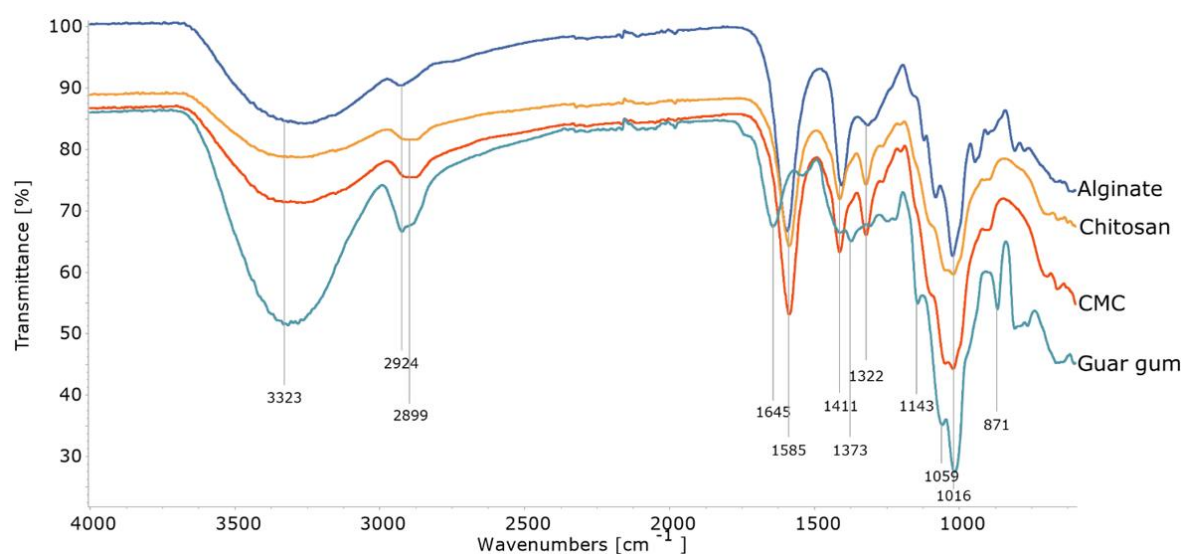

Figure 3. FTIR spectra of the individual polymers: alginate, chitosan, CMC, and guar gum.

Hydrogel C25A50X12.5G12.5 consistently shows low swelling performance at both pH 2 and pH 6.8, while hydrogel C50A25X25 is among those that have the highest swelling performance. All of the hydrogels show an increase in swelling ratio in pH 6.8 phosphate buffer at 2 h, which is higher than the increase at pH 2. At 24 h of incubation, all hydrogels were digested.

Based on the swelling performance test, hydrogels C50A25X25, C25A50X25, C25A50G25, C25A25G50, C25A50X12.5G12.5, and C25A25X25G25 are not digested at pH 2 but digested at pH 6.8. These results indicate that these formulas are suitable for nutrient delivery to the intestinal area. These hydrogels have a high chance of protecting the nutrients from the digestion of gastric juice, which has a low pH.

Moreover, the hydrogels show minimum swelling (less than 3x) under physiological pH, which indicates that the hydrogels retain their shape at least for the first two hours at pH 2 and pH 6.8 (Tang *et al*., 2021).

Fourier-transform infrared spectroscopy (FTIR)

The FTIR spectra of the individual polymers that were used to produce the hydrogel (Figure 3) As all polymers contain hydroxyl groups (O–H), a strong and broad peak for the stretching vibration at 3323 cm^{-1} distinguishes intermolecular bonded hydroxyl groups. The medium and sharp peak of the free hydroxyl group at around 3700 cm^{-1} is missing, suggesting that the O–H was involved in a hydrogen bond.
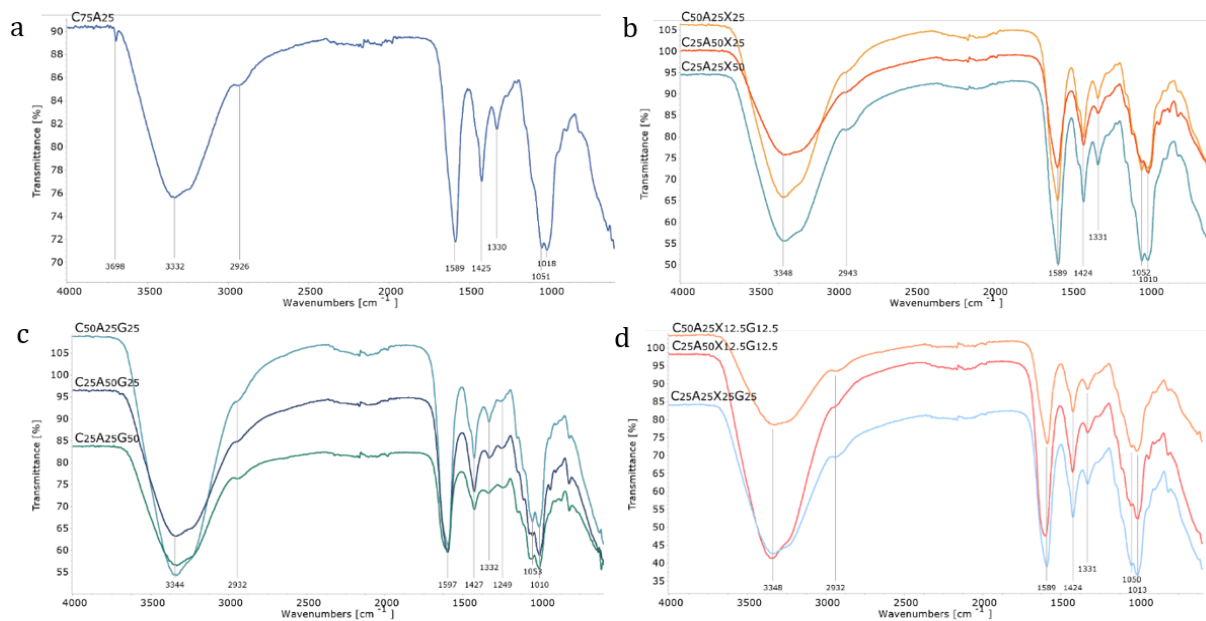
Figure 4 FTIR spectra of dry hydrogel produced with CMC-alginate (a), CMC-alginate-chitosan (b), CMC-alginate-guar gum (c), and CMC-alginate-chitosan-guar gum (d). C=CMC, A=alginate, X=chitosan, G=guar gum.
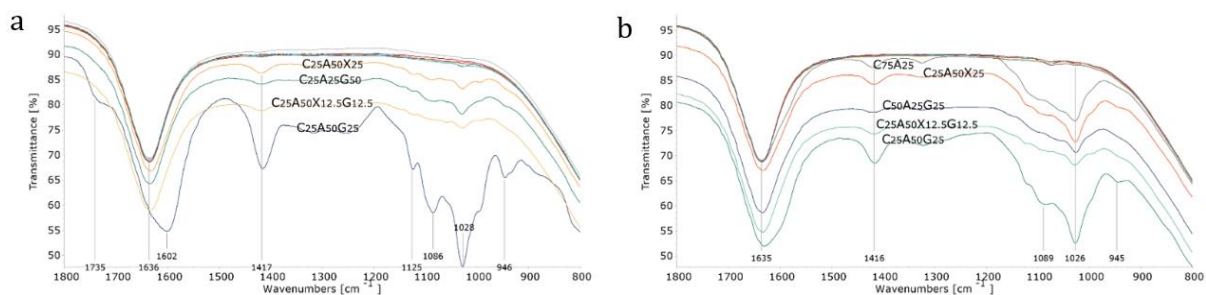

Figure 5. FTIR spectra of hydrogel immersed in HCl buffer pH 2 (a) and phosphate buffer pH 6.8 (b) until reaching equilibrium.

While chitosan is the only polymer with the N–H group, the peak at around 3500 cm^{-1} was obscured by the broad O–H peak. A medium peak at 2924-2899 cm^{-1} corresponds to C–H stretching and is present in all spectra. In guar gum, O–H bending due to water molecules was visible at 1645 cm^{-1} (Iqbal, Nazir, Iqbal, & Yameen, 2020). The strong peak at 1585 cm^{-1} is attributed to C=O stretching in CMC, alginate, and chitosan. While not having C=O in its molecule, chitosan may retain C=O from the residual chitin that is not completely deacetylated during the formation of chitosan (Queiroz *et al*., 2014). In the region of 1500-1300 cm^{-1}, all polysaccharides have several peaks which correspond to C–H bending. The peak at 1143 cm^{-1} is attributed to C–N stretching of amine, while peaks at 1059 cm^{-1}

and 1016 cm^{-1} are C–O stretching of the several groups that are present in the polymers.

The combinations of two to four types of polysaccharides retain most of the features of the individual polymers in the FTIR spectra of the freeze-dried hydrogels (Figure 4). Most of the successfully made hydrogels have similar patterns in the FTIR spectra, with minor differences. A convoluted broad band at around 3340 cm^{-1} indicated a combination of the inter- and intramolecular O–H bonds formed during polymerizations (Kondo, 1997). An indication of free hydroxyl group, due to rearrangement of the molecules during reaction mixtures (Kondo, 1997), appears weakly at 3698 cm^{-1} in the FTIR spectra of C75A25.
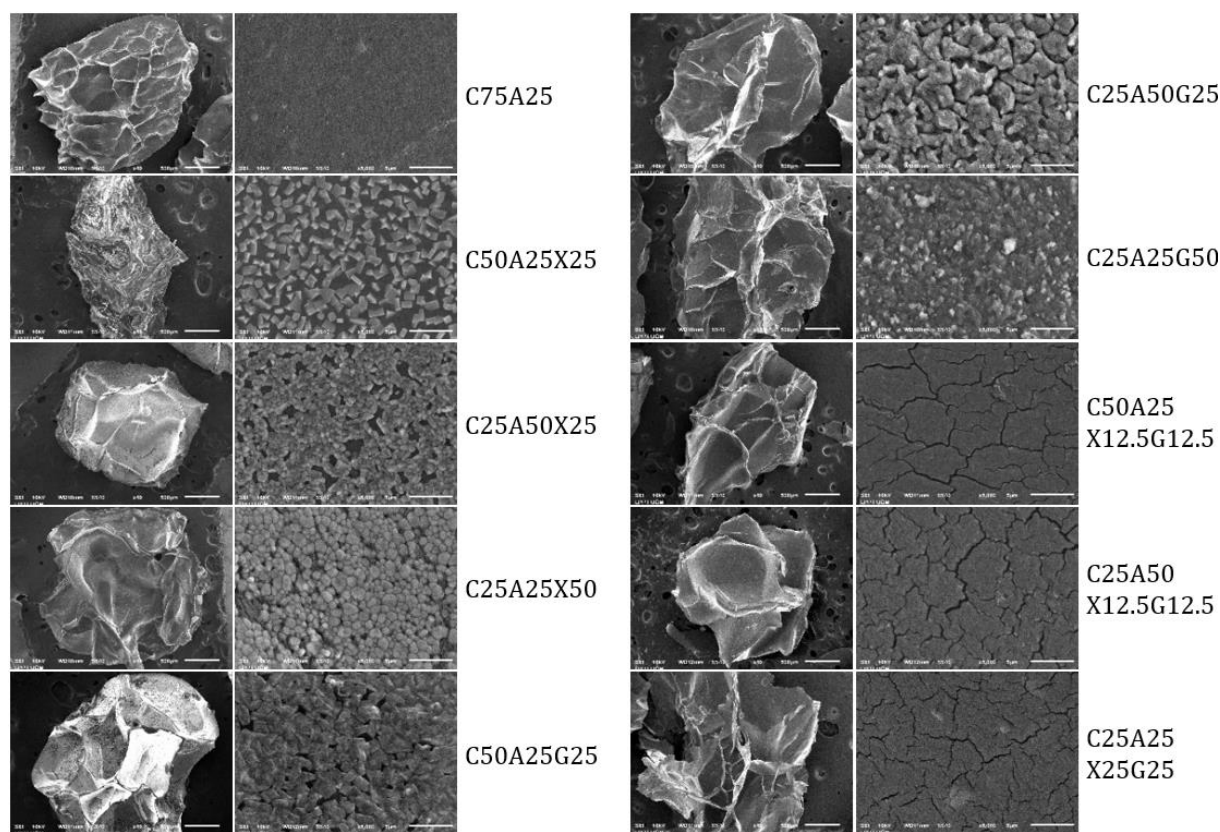
Figure 6 SEM imaging of dry hydrogels for each formula with 40× magnification (left picture) and 5000× magnification (right picture). C=CMC, A=alginate, X=chitosan, G=guar gum.

Crosslinking causes the C–H stretching in the mixture to appear weaker than in individual polymers (Yaghoubi *et al.*, 2021). Absent in other spectra, the peak weakly appearing at 1249 cm^{-1} in CMC-alginate-guar gum hydrogels resembles C–H bending, which may come from guar gum as these mixtures contain a high percentage of guar gum.

The crosslinking behavior of the hydrogels in simulated stomach solution was investigated using hydrochloric acid-potassium chloride buffer at pH 2. The FTIR spectra of all formulas show a broad O–H peak at around 3300 cm^{-1} (figure not shown) and a strong peak at 1636 or 1602 cm^{-1}, which is the characteristic of C=O stretching (Figure 5A). Hydrogel C25A50G25 has a characteristic peak at 1735 cm^{-1}, which indicates protonated C=O involved in hydrogen bond (Barbucci *et al.*, 2000). The hydrogen bond is further evidenced by the C=O peak of amide at 1602 cm^{-1}. For the fingerprint area, hydrogels C25A50X25, C25A25G50, and C25A50X12.5G12.5 show weak peaks at 1417 cm^{-1} and 1028 cm^{-1}, which correspond to C–H bending and C–O stretching, respectively. Hydrogel C25A50G25 has strong peaks at 1417 cm^{-1} and 1028 cm^{-1}, with additional weak to medium peaks at 1125, 1086, and 946 cm^{-1}. The higher intensity of the C–H band indicates stronger crosslinking of the hydrogel, in addition to the abundance of hydrogen bonds (Barbucci *et al.*, 2000).

The FTIR spectra were produced from hydrogels immersed in phosphate buffer at pH 6.8 to simulate intestinal fluid. Similar to those at pH 2, a broad band at around 3300 cm^{-1} of O–H peak indicates the presence of hydrogen bonding in all formulas (figure not shown). A strong peak at 1635 cm^{-1} of C=O stretching is observed in all hydrogels (Figure 5B). Only hydrogel C75A25, C25A50X25, C50A25G25, C25A50G25, and C25A50X12.5G12.5 exhibit a weak band of C-H bending at 1416 cm^{-1}. Those formulas also show a strong peak at 1026 cm^{-1} of C–O stretching. Hydrogel C25A50G25 has additional bands at 1089 cm^{-1} and 945 cm^{-1}, which are also visible when the hydrogel is immersed in pH 2.

Scanning electron microscopy (SEM)

The morphology of the surface of the hydrogel was depicted using SEM imaging (Figure 6). In general, all beads are of irregular round shape with a diameter of around 1,5 mm. The hydrogel C75A25, composed of CMC and alginate, shows a homogenous surface, which indicates that the calcium chloride was well-dispersed. The negatively charged CMC and alginate will form ionic interaction with Ca^{2+} during the crosslinking to form the gel-like structure (Hu *et al.*, 2019). In contrast, the calcium chloride in hydrogel C50A25X25 was visible, indicating inefficient cross-linking. The addition of positively charged chitosan may not be well-dispersed during the hydrogel formation, as it can form electrostatic interaction with Ca^{2+} or other anionic polyelectrolytes (Hu *et al.*, 2019). Hydrogel C25A50X25, C25A25X50, C50A25G25, and C25A50G25 have granular-liked structures that loosely linked to one another (Miller & Peppas, 1986), due to the water sublimation during the freeze-drying process. The surface of hydrogel C25A25G50 indicates compact cross-linking (Hezaveh & Muhamad, 2012).

The hydrogel C50A25X12.5G12.5, C25A50X12.5G12.5, and C25A25X25G25 show cracking phenomena on the dense surface of the hydrogel, as seen in the SEM result. The dense surface indicates higher polymerization of the hydrogel, while the freeze-drying process enhances this feature (Bialik-Wąs *et al.*, 2021). The cracks appear due to water sublimation during the preparation process. Hydrogels absorb water molecules inside their structure, and sudden freezing temperature sublime the water and leave a crack in the dry structure. This phenomenon was previously observed in alginate hydrogel with calcium chloride as the cross-linking solution (Aston *et al.*, 2016).

Incorporation of active ingredients, both in terms of drugs or supplements, into hydrogel will be beneficial for controlling drug delivery and increasing stability. Peptides and proteins are now being developed to be more stable for oral administration, by incorporating them into a suitable hydrogel shell. Peptide has been successfully incorporated in chitosan-based hydrogel for oral delivery, in which gastrointestinal absorption can be facilitated due to the pH suitability (Wong *et al.*, 2018), in agreement with our result. Alginate-based hydrogel crosslinked using calcium carbonate and d-glucono-δ-lactone is potentially used as wound dressing for dermal therapy containing vitamin D_3 (Ehterami *et al.*, 2020). Therefore, the implementation of hydrogel for drug and supplement delivery ranges widely, both in terms of active ingredients content and route of administration.

CONCLUSION

The combination of natural polymers with different ratios of CMC, alginate, chitosan, and/or guar gum was successfully made into hydrogels with $CaCl_2$ as a crosslinker. The hydrogels formed were characterized using FTIR and SEM, which reveal distinguishable features between formulations. Swelling test were done at pH 2 and 6.8 to evaluate the hydrogel performance in simulated gastrointestinal fluid. Six of the formulas were not digested at pH 2 but digested at pH 6.8 during the first two hours of the swelling test, indicating that the formulas were suitable for nutrients or drug deliveries to the intestine. This study provides a starting guide for the formulation of hydrogel as a vehicle for nutrient delivery in the gastrointestinal track. Further studies which involve each type of active ingredients (e.g., probiotics, vitamin, mineral, protein, etc.) should be performed to evaluate hydrogel performance containing active ingredients. Further analysis of hydrogel characteristics, such as using texture analyzer and thermal characterization, can be used to evaluate beads quality and understand the interpolymer interaction.

CONFLICT OF INTEREST

The authors declare that there is no competing interest.

REFERENCES

Aston, R., Sewell, K., Klein, T., Lawrie, G., & Grøndahl, L. (2016). Evaluation of the impact of freezing preparation techniques on the characterisation of alginate hydrogels by cryo-SEM. *European Polymer Journal*, *82*, 1–15. https://doi.org/10.1016/j.eurpolymj.2016.06.025

Azeera, M., Vaidevi, S., & Ruckmani, K. (2019). Characterization Techniques of Hydrogel and Its Applications. In M. Mondal (Ed.), *Cellulose-Based Superabsorbent Hydrogels*

(pp. 737–761). https://doi.org/10.1007/978-3-319-77830-3_25

Barbucci, R., Magnani, A., & Consumi, M. (2000). Swelling behavior of carboxymethylcellulose hydrogels in relation to cross-linking, pH, and charge density. *Macromolecules*, *33*(20), 7475–7480. https://doi.org/10.1021/ma0007029

Bialik-Wąs, K., Królicka, E., & Malina, D. (2021). Impact of the Type of Crosslinking Agents on the Properties of Modified Sodium Alginate/Poly(vinyl Alcohol) Hydrogels. *Molecules*, *26*(8), 2381. https://doi.org/10.3390/molecules26082381

Çelik, E., Bayram, C., Akçapınar, R., Türk, M., & Denkbaş, E. B. (2016). The effect of calcium chloride concentration on alginate/Fmoc-diphenylalanine hydrogel networks. *Materials Science and Engineering: C*, *66*, 221–229. https://doi.org/10.1016/j.msec.2016.04.084

Ehterami, A., Salehi, M., Farzamfar, S., Samadian, H., Vaez, A., Sahrapeyma, H., & Ghorbani, S. (2020). A promising wound dressing based on alginate hydrogels containing vitamin D3 cross-linked by calcium carbonate/d-glucono-δ-lactone. *Biomedical Engineering Letters*, *10*(2), 309–319. https://doi.org/10.1007/s13534-020-00155-8

Fernandes Queiroz, M., Melo, K., Sabry, D., Sassaki, G., & Rocha, H. (2014). Does the Use of Chitosan Contribute to Oxalate Kidney Stone Formation? *Marine Drugs*, *13*(1), 141–158. https://doi.org/10.3390/md13010141

Feyissa, Z., Edossa, G. D., Gupta, N. K., & Negera, D. (2023). Development of double crosslinked sodium alginate/chitosan based hydrogels for controlled release of metronidazole and its antibacterial activity. *Heliyon*, *9*(9), e20144. https://doi.org/10.1016/j.heliyon.2023.e20144

H. Gulrez, S. K., Al-Assaf, S., & O, G. (2011). Hydrogels: Methods of Preparation, Characterisation and Applications. In A. Carpi (Ed.), *Progress in Molecular and Environmental Bioengineering - From Analysis and Modeling to Technology Applications*. https://doi.org/10.5772/24553

Hezaveh, H., & Muhamad, I. I. (2012). Impact of metal oxide nanoparticles on oral release properties of pH-sensitive hydrogel nanocomposites. *International Journal of Biological Macromolecules*, *50*(5), 1334–1340. https://doi.org/10.1016/j.ijbiomac.2012.03.017

Hu, W., Wang, Z., Xiao, Y., Zhang, S., & Wang, J. (2019). Advances in crosslinking strategies of biomedical hydrogels. *Biomaterials Science*, *7*(3), 843–855. https://doi.org/10.1039/C8BM01246F

Iqbal, D. N., Nazir, A., Iqbal, M., & Yameen, M. (2020). Green synthesis and characterization of carboxymethyl guar gum: Application in textile printing technology. *Green Processing and Synthesis*, *9*(1), 212–218. https://doi.org/10.1515/gps-2020-0022

Ji, D., Park, J. M., Oh, M. S., Nguyen, T. L., Shin, H., Kim, J. S., … Kim, J. (2022). Superstrong, superstiff, and conductive alginate hydrogels. *Nature Communications*, *13*(1), 3019. https://doi.org/10.1038/s41467-022-30691-z

Kondo, T. (1997). The assignment of IR absorption bands due to free hydroxyl groups in cellulose. *Cellulose*, *4*(4), 281–292. https://doi.org/10.1023/A:1018448109214

Liu, K., Chen, Y.-Y., Zha, X.-Q., Li, Q.-M., Pan, L.-H., & Luo, J.-P. (2021). Research progress on polysaccharide/protein hydrogels: Preparation method, functional property and application as delivery systems for bioactive ingredients. *Food Research International*, *147*, 110542. https://doi.org/10.1016/j.foodres.2021.110542

Miller, D. R., & Peppas, N. A. (1986). Bulk characterization and scanning electron microscopy of hydrogels of P(VA-co-NVP). *Biomaterials*, *7*(5), 329–339. https://doi.org/10.1016/0142-9612(86)90003-7

Mun, S., Kim, Y. R., & McClements, D. J. (2015). Control of β-carotene bioaccessibility using starch-based filled hydrogels. *Food Chemistry*, *173*, 454–461. https://doi.org/10.1016/j.foodchem.2014.10.053

Pak, S., & Chen, F. (2023). Functional Enhancement of Guar Gum–Based Hydrogel by Polydopamine and Nanocellulose. *Foods*,

12(6), 1304. https://doi.org/10.3390/foods12061304

Panahi, R., & Baghban-Salehi, M. (2019). Protein-Based Hydrogels. In M. I. H. Mondal (Ed.), *Cellulose-Based Superabsorbent Hydrogels* (pp. 1561–1600). https://doi.org/10.1007/978-3-319-77830-3_52

Rahman, M. S., Islam, M. M., Islam, M. S., Zaman, A., Ahmed, T., Biswas, S., … Rahman, M. M. (2019). *Morphological Characterization of Hydrogels.* https://doi.org/10.1007/978-3-319-77830-3_28

Tang, R.-C., Chen, T.-C., & Lin, F.-H. (2021). Design Strategy for a Hydroxide-Triggered pH-Responsive Hydrogel as a Mucoadhesive Barrier to Prevent Metabolism Disorders. *ACS Applied Materials & Interfaces*, *13*(49), 58340–58351. https://doi.org/10.1021/acsami.1c17706

Trombino, S., Cassano, R., Bloise, E., Muzzalupo, R., Tavano, L., & Picci, N. (2009). Synthesis and antioxidant activity evaluation of a novel cellulose hydrogel containing trans-ferulic acid. *Carbohydrate Polymers*, *75*(1), 184–188. https://doi.org/10.1016/j.carbpol.2008.05.018

Wong, C. Y., Al-Salami, H., & Dass, C. R. (2018). The role of chitosan on oral delivery of peptide-loaded nanoparticle formulation. *Journal of Drug Targeting*, *26*(7), 551–562. https://doi.org/10.1080/1061186X.2017.1400552

Yaghoubi, A., Ramazani, A., & Ghasemzadeh, H. (2021). Synthesis of physically crosslinked

PAM/CNT flakes nanocomposite hydrogel filmsviaa destructive approach. *RSC Advances*, *11*(62), 39095–39107. https://doi.org/10.1039/d1ra07825a

Zhang, Z., Zhang, R., Decker, E. A., & McClements, D. J. (2015). Development of food-grade filled hydrogels for oral delivery of lipophilic active ingredients: PH-triggered release. *Food Hydrocolloids*, *44*, 345–352. https://doi.org/10.1016/j.foodhyd.2014.10.002

Zhang, Z., Zhang, R., & McClements, D. J. (2016). Encapsulation of β-carotene in alginate-based hydrogel beads: Impact on physicochemical stability and bioaccessibility. *Food Hydrocolloids*, *61*, 1–10. https://doi.org/10.1016/j.foodhyd.2016.04.036

Zhang, Z., Zhang, R., Zou, L., Chen, L., Ahmed, Y., Al Bishri, W., … McClements, D. J. (2016). Encapsulation of curcumin in polysaccharide-based hydrogel beads: Impact of bead type on lipid digestion and curcumin bioaccessibility. *Food Hydrocolloids*, *58*, 160–170. https://doi.org/10.1016/j.foodhyd.2016.02.036

Zhang, Z., Zhang, R., Zou, L., & McClements, D. J. (2016). Protein encapsulation in alginate hydrogel beads: Effect of pH on microgel stability, protein retention and protein release. *Food Hydrocolloids*, *58*, 308–315. https://doi.org/10.1016/j.foodhyd.2016.03.015